JEE Journal of Ecological Engineering

Journal of Ecological Engineering, 2025, 26(1), 30–45
https://doi.org/10.12911/22998993/195214
ISSN 2299–8993, License CC-BY 4.0

Received: 2024.10.02
Accepted: 2024.11.15
Published: 2024.12.01

Experimental study of carbon dioxide capture and mineral carbonation using sodium hydroxide solution

Ruey-Yu Chan[1*], Yu-Zhen Zeng[1], Chun-Chi Hou[1], Hsian-Cang Kou,Huang-Wei Huang[1]

[1] Chemical Engineer Division, National Atomic Nuclear Research Institute, No. 1000, Wenhua Rd., Longtan Dist., Taoyuan City 325207, Taiwan (R.O.C.)
* Corresponding author's e-mail: rychan@nari.org.tw

ABSTRACT

The mineral carbonation process was proposed for effective CO_2 capture and utilization from flue gas streams, such as those emitted by coal-fired power plants. In the present work, an alternative technology using sodium hydroxide (NaOH) solution as an absorbent for capturing CO_2 and converting it into value-added materials while mitigating emissions was provided. This research examined the use of a packed bed reactor and a bubble column reactor for CO_2 absorption and carbonation of NaOH solution to produce sodium bicarbonate ($NaHCO_3$), offering a more environmentally friendly production process compared to traditional methods. The influence of significant operating parameters, namely pH value, gas flow rate, and absorbent flow rate, on CO_2 capture in a bubble column reactor was experimentally explored using NaOH solution. The formation of sodium bicarbonate during the carbonation experiment was confirmed by X-ray diffraction (XRD) and thermal gravimetric analysis (TGA). The experimental results show a CO_2 removal efficiency exceeding 95% and a $NaHCO_3$ purity above 94% when utilizing a bubble column reactor.

Keywords: CO_2 capture, sodium hydroxide, packed bed reactor, bubble column reactor.

INTRODUCTION

The increasing concern over climate change highlights significant and enduring alterations in Earth's climate patterns over extended periods. One of the primary manifestations of climate change is the observed rise in global average temperatures, which is largely attributed to the excessive accumulation of greenhouse gases (GHGs) in the atmosphere. Among these gases, carbon dioxide (CO_2) is notably prevalent, contributing to a warming phenomenon, commonly referred to as global warming. The ramifications of climate change result in a myriad of environmental issues, including an escalation in extreme weather occurrences and sea level elevation. These environmental challenges are primarily triggered by human activities, such as burning fossil fuels for energy, industrial processes, and deforestation, contributing significantly to the surge in greenhouse gas emissions. To limit the rise in global mean temperature to below the originally projected 1.5 °C, a 45% reduction in global CO_2 emissions by 2030 and the achievement of net zero emissions by 2050 are crucial [1]. Carbon dioxide capture encompasses various technologies that capture CO_2 at different stages, including post-combustion capture, pre-combustion capture, and oxy-fuel combustion. In traditional carbon dioxide capture and utilization (CCS) processes, the amine absorption method stands as the prevailing technique for CO_2 capture [2–4]. Nonetheless, it faces challenges like toxicity, degradation, high energy requirements for absorbent regeneration, and susceptibility to impurities.

An alternative absorbent for CO_2 capture is sodium hydroxide (NaOH), which is more environmentally friendly, eliminates the cost associated with pre-treatment, and requires milder process parameters than other competing carbon capture processes. Carbon dioxide capture and

utilization (CCU) stands out as a promising solution for reducing the current CO_2 emissions stemming from fossil fuel usage. Once captured, CO_2 can be transformed into valuable products such as carbonate products, chemicals, fuels, polymers, and plastics. In the realm of CO_2 capture and utilization, carbonation emerges as an alternative process for capturing CO_2 from flue gas and converting it into high-value materials [5]. This technology not only aids in lowering the CO_2 emissions but also transforms a challenge into an opportunity by utilizing CO_2 to create raw materials for diverse applications.

While the CO_2 capture by the carbonation of sodium hydroxide solution is straightforward conceptually, the mechanism of the carbonation reaction is intricate due to its three-phase (gas-liquid-solid) reactions [6-9]. When CO_2 interacts with sodium hydroxide solution, two distinct reactions occur. Initially, the combination of NaOH and CO_2 produces sodium carbonate (Na_2CO_3) and water (H_2O) with the release of -169.8 kJ (Equation 1). Subsequently, the formed sodium carbonate further reacts with CO_2 and water to yield two molecules of sodium bicarbonate ($NaHCO_3$) with the release of -129.1 kJ (Equation 2). The overall conversion involves the reaction of two molecules of NaOH and two molecules of CO_2 to result in the formation of two molecules of sodium bicarbonate (Equation 3). This series of reactions demonstrates the transformation of reactants into valuable bicarbonate products through the carbonation process.

$$2NaOH_{(aq)} + CO_{2(g)} \rightarrow \rightarrow Na_2CO_{3\,(aq)} + H_2O_{(l)}\,\Delta H = -169.8 \quad (1)$$

$$Na_2CO_{3(aq)} + CO_{2(g)} + H_2O_{(l)} \rightarrow \rightarrow 2NaHCO_{3(s)}\,\Delta H = -129.1 \quad (2)$$

Overall reaction

$$2NaOH_{(aq)} + 2\,CO_{2(g)} \rightarrow 2NaHCO_{3(s)} \quad (3)$$

From a thermodynamic perspective, this process offers key advantages, as it is thermodynamically favorable and requires relatively less energy, particularly due to operating at near-room temperatures and atmospheric pressure. When utilizing a NaOH aqueous solution as an absorbent to capture CO_2, it typically undergoes conversion into $NaCO_3$ before entering the carbonation process. This preliminary conversion step is necessary due to the sluggish reaction kinetics of carbonation. However, the slow kinetics of carbonation can pose practical challenges in the chemisorption of CO_2 within NaOH solutions, leading to reduced capture capacity and necessitating larger capture plant sizes. To address this issue and enhance reaction kinetics, gas-liquid bubble columns are being designed. These reactors aim to achieve more cost-effective capture rates by facilitating more efficient interaction between CO_2 and the NaOH solution in the bubble column system.

In this research, an aqueous carbonation process was developed to capture CO_2 from flue gas streams, particularly emissions from sources like coal-fired power plants, and transform the CO_2 into valuable materials. Bench-scale experiments were conducted to assess key parameters, such as pH value, gas flow rate, and liquid flow rate, by utilizing NaOH alkaline solution as the absorbent. The experimental exploration aimed to quantify the efficiency of CO_2 capture under varying conditions. In the ongoing development of this research, the focus was on scaling up the process. A pilot-scale unit was expanded and designed to capture CO_2 from a slipstream of flue gas derived from a heavy oil steam boiler. This scale-up aimed to demonstrate the viability and effectiveness of the aqueous carbonation process on a larger scale and under conditions more akin to industrial settings.

EXPERIMENTAL WORK

The study investigated the optimal process conditions for CO_2 mineral carbonation in a semi-batch reactor by examining various parameters such as pH value, gas flow rate, and liquid flow rate. Carbonation performance in a bubble column reactor was evaluated based on CO_2 removal efficiency and $NaHCO_3$ purity.

Chemicals

All chemicals used in this study were purchased directly from vendors without any additional purification steps. Sodium hydroxide (≥ 98% assay) was sourced from Merck Chemicals Taiwan, while analytical grade CO_2 and N_2 (> 99.9% purity) were obtained from San Fu Chemical CO. to mimic flue gas conditions. A 15 wt% NaOH aqueous solution with an initial pH of 14 served as the absorbent for CO_2 capture, prepared by diluting NaOH pellets in deionized water. The simulated flue gas, composed of 15 vol% CO_2, was adjusted with N_2 gas to replicate emissions from fossil fuel-fired plants.

Experimental apparatus

In the experiments focusing on the removal of CO_2 using NaOH solution, a semi-batch reactor setup was utilized. The packed bed column was made of stainless steel with 60 mm inside diameter and 1500 mm height. The total packing height was 1100 mm, comprising metallic Pall rings with a diameter of 16 mm. The packing layer's void fraction was 93%, and it had a surface area of approximately 316 m^2/m^3. Simulated flue gas was introduced into the reactor at a volume flow rate ranging from 300 to 700 L/h, while the NaOH solution flow rate varied from 3 to 20 L/h. Operating in semi-batch mode, the absorbent solution was pumped to the top of the columns and descended through the packing under gravity, interacting with the simulated flue gas entering at the column's base in a counter-current manner. Furthermore, the experimentation was extended to CO_2 capture and mineralization via sodium hydroxide absorption in a bubble column reactor (BCR). The bubble column, fabricated from stainless steel, featured an internal diameter of 0.2 m and a height of 1.2 m. A hemisphere bubble diffuser with a pore size of 10 μm and a surface area of 353 cm^2 was fitted at the bottom of the column to maintain a steady, uniformly dispersed bubble flow within the liquid phase. Design specification and its characteristics of the bench-scale experimenter are summarized in Table 1.

In these experiments, simulated flue gas was introduced into the reactor at 500 L/h, interacting with 2 L of absorbent liquid maintained at a height of 15 mm above the bubble diffuser. The gas exiting the top of the column underwent measurement using a non-dispersive infrared-based CO_2 analyzer before being purged. The experimental setup depicted in Figure 1 illustrated the carbonation process of NaOH solution for carbon capture and utilization. Various process parameters, such as solution pH, gas flow rate, and absorbent

Figure 1. Photo of bench-scale experiments for CO_2 captured and mineral carbonation in NaOH. solution: 1 –bubble column reactor, 2 – packed bed reactor, 3 – NaOH solution tank, 4 – CO_2 analyzer, 5 – pH meter, 6 –instrument indicator, 7 – absorbent inlet flow, 8 – CO_2 inlet flow

Table 1. Reactor characteristics of bench-scale experimenter for CO_2 captured and mineral carbonation

Specifications	Reactor	
	Packed bed reactor	Bubble column reactor
Height /Diameter (m)	1.5 /0.06	1.2/0.2
Column walls material	S.S 304	S.S 304
Packing material	Raschig rings	-
Raschig rings dimensions	Pall rings (16 × 16 mm)	-
Packing material	Raschig rings	-
Bubble diffuser	-	Gas spargers*

Note: *Four gas spargers were used in bubble column reactor.

flow rate were investigated to identify the optimum conditions for CO_2 mineral carbonation in a semi-batch reactor.

Material characterization

In CO_2 mineral carbonation experiments, the absorbent solution may contain three chemical species: OH^-, CO_3^{2-} and HCO_3^-, which depend on the pH values. The concentrations of carbonate species allows determining the CO_2 removal efficiency in absorbent solution. To analyze the species concentration in the absorbent, the double indicators method was used. Two base indicators, such as phenolphthalein (PP) and methyl orange (MO), are employed to identify the products like sodium carbonate and sodium bicarbonate, respectively. The sample, which is alkaline, was titrated with HCl and two indicators that change color and indicate what species is in solution during titration.

The sample, which is alkaline, undergoes titration with HCl using two indicators that change color to indicate the species present in the solution. Phenolphthalein was initially added to the sample, turning it purple. HCl was then added drop by drop until the solution becomes colorless, signifying the presence of only bicarbonate in the solution after an HCl volume of V_1 has been added. Following this, Methyl orange was added to the sample, turning it yellow. HCl was once more added drop by drop until the solution turned pink after adding another volume V_2 of HCl, indicating that all bicarbonates have reacted to form H_2CO_3.

The reactions involved are:

$$Na_2CO_3 + HCl \rightarrow NaHCO_3 + NaCl \quad (4)$$

$$NaHCO_3 + HCl \rightarrow NaCl + H_2O + CO_2 \quad (5)$$

The presence of reaction (4) is indicated by phenolphthalein, while the occurrence of reaction (5) is signaled by methyl orange. The volumes of hydrochloric acid consumed during the titration process in the presence of phenolphthalein and methyl orange are represented as V_1 and V_2, respectively. After the mineral carbonation, the carbonates precipitated from the experiments were filtered to isolate the precipitated cake, which was then thoroughly dried at 50 °C in a vacuum oven. The powdered carbonate produced by the mineralization processes was analyzed with X-ray diffraction (XRD) for phase detection and the purity of $NaHCO_3$ was also measured using thermogravimetric analysis (TGA) results. The X-ray diffraction patterns of the solid samples were captured using a Siemens XRD D8 Monochromatic Diffractometer, which is outfitted with CuKa (λ = 1.54 Å) radiation at a beam voltage of 40 kV. The XRD patterns were recorded in the range of 20 to 80° with a step size of 0.02° and a scan rate of 1°/min. These analyses were conducted to elucidate the crystal structure of the carbonate precipitates. Thermo-gravimetric analyses were conducted using a thermal TGA Q500, TA Instrument. The samples were placed in an alumina crucible and heated at a rate of 10 °C /min from room temperature to 900 °C in N_2 flow. The first derivative of the TG curve was also determined to assist the calculation of the weight loss occurred during the heating process. The weight loss in the temperature region of 90–190 °C was determined to be the decomposition of $NaHCO_3$.

RESULTS AND DISCUSSION

CO_2 absorption and carbonation in NaOH solution

The mineral carbonation reaction of CO can be divided into distinct individual steps. This study experimentally investigates the gas-liquid-solid multiphase reaction. Initially, gaseous

CO_2 is absorbed in a high-pH caustic solution, forming carbonic acid, which then further ionize into hydrogen ions (H^+) and carbonate ions (CO_3^{2-}), thereby promoting the carbonation reaction to produce sodium carbonate and sodium bicarbonate. Once the absorbent solution is saturated with the CO_2 gas, it can no longer absorb more carbon dioxide, indicating the end of CO_2 absorption, followed by the carbonation reaction. As the reaction progresses, the absorbed CO_2 reacts with carbonate ion to produce carbonate, and then the bicarbonate formation proceeds according to reaction (3) and (4), respectively. Eventually, as the bi-carbonation process slowly proceeds during bi-carbonation, the amount of sodium bicarbonate precipitated in the liquid phase gradually increases.

All experiments were conducted in semi-batch mode, using 14 wt% NaOH solution with an initial pH of 13.93 as the absorbent, and then injecting 15 vol% CO_2 to simulate flue gas into the reactor. The laboratory-scale experiments aimed to determine the optimal conditions for CO_2 absorption and carbonation in the NaOH solution. The study further analyzed the absorption of CO_2 by the NaOH solution to compare its efficiency in capturing CO_2.

When CO_2 is injected into a constant amount of the NaOH absorbent, sodium hydroxide reacts with the absorbed CO_2 to generate sodium carbonate and sodium bicarbonate according to reactions (1) and (2), respectively. As depicted in Figure 2, the solution pH serves as a major indicator of the progress of CO_2 absorption and carbonation in the NaOH solution. Initially, due to the low amount of absorbed CO_2, only a small amount of hydroxide ions (OH^-) is consumed, leading to a slow decrease in the pH value of the solution. After about one hour, the pH gradually drops from 13.93 to 13.25. As illustrated in Figure 2, as absorption progresses, more absorbed CO_2 gas reacts with OH^- to form intermediate sodium carbonate, further reducing the pH value of the solution. As depicted in Figures 2 and 3, during this phase, the pH value exhibits minimal change due to the relatively high concentration of OH^- in the absorbent solution, indicating a relatively high CO_2 removal efficiency. The absorption experiments lasted approximately two hours, during which the initial pH dropped from 13.93 to 10.92, while the CO_2 removal efficiency decreased significantly. As observed in Figure 3, at a pH value of 10, the minimum capture efficiency was only 10%. As the reaction progressed, the pH-value was little changed because of relatively low concentration of the OH^- available in absorbent solution and consequently bicarbonate ions ($HCOH_3^-$) become the main constituent.

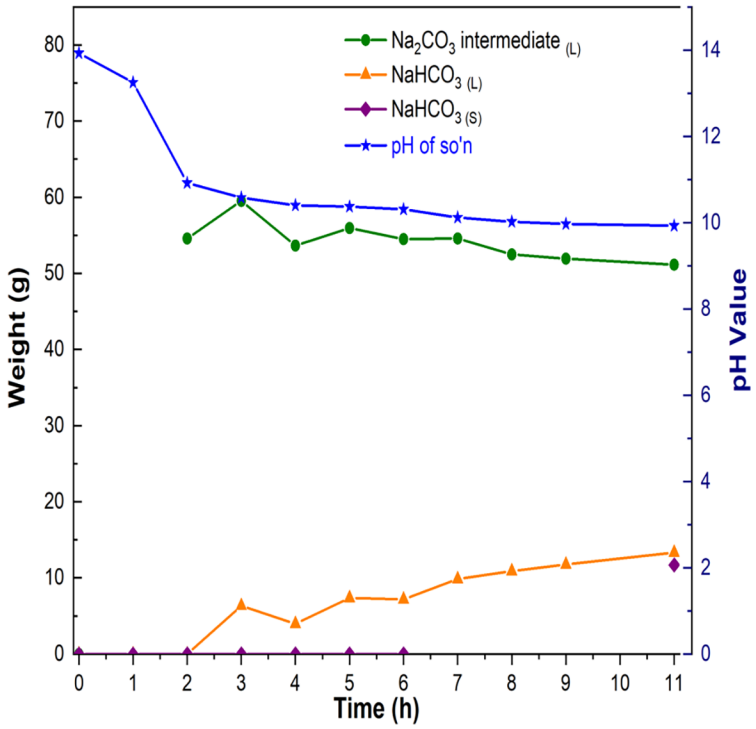

Figure 2. Variation of carbonate species and pH value during the carbonation in NaOH solution

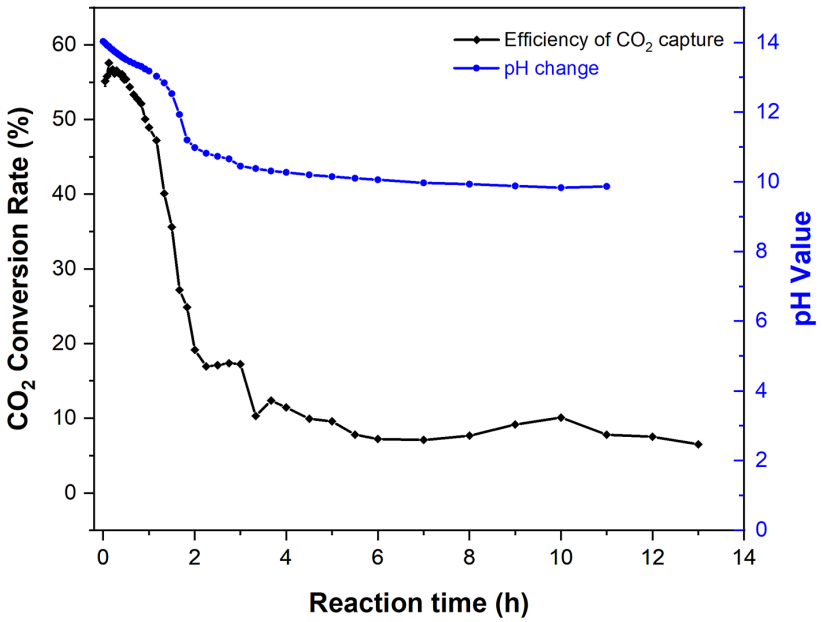

Figure 3. Variation of CO_2 removal efficiency and pH value during the carbonation in NaOH solution

As depicted in Figure 2, after two hours, the concentration of Na_2CO_3 in the solution exceeded 25.7 wt% (59.5 g), while the concentration of bi-carbonate ions in the liquid phase is negligible. After about three hours of reaction, the absorbed CO_2 gas reacts with the remaining carbonate ions in the solution, initiating the bi-carbonation reaction. Due to the slow reaction rate, there was only a small amount of $NaHCO_3$ in the absorbent, with approximately 2.7 wt% of aqueous $NaHCO_3$ in the solution. About six hours after the start of the reaction, the concentration of $NaHCO_3$ exceeded its saturation point at that temperature, leading to the formation of $NaHCO_3$ crystal precipitation. As the reaction continued, the absorbed CO_2 further reacted with the carbonate ions to form the $NaHCO_3$ precipitate, extending the time for $NaHCO_3$ precipitation as bicarbonate ions and CO_2 became further saturated. Approximately 11 hours after the start of the reaction, the precipitated $NaHCO_3$ reached its maximum yield. Eventually, the absorbent solution became fully saturated and could no longer absorb more CO_2. At the end of the reaction, the precipitated $NaHCO_3$ was dehydrated and dried, yielding pure $NaHCO_3$ with a total weight of approximately 11.7 g (5.6 wt%).

Characterization of synthesized precipitant $NaHCO_3$ precipitation

Simulated flue gas is fed to a packed bed reactor, where a aqueous NaOH solution reacts counter currently with the CO_2 from the flue gas. During the absorption process, the absorbed CO_2 in NaOH solution instantly converted into Na_2CO_3 (Reaction 2). Then, the Na_2CO_3 solution slowly reacted with simulated flue gas to yield the $NaHCO_3$ crystals (Reaction 3). After the $NaHCO_3$ solution had reached saturated concentration, the crystallization of precipitated $NaHCO_3$ started to form.

All of the synthesized precipitates from the experiments were completely dried at 50 °C in a vacuum oven and were characterized. To investigate the properties of the precipitated $NaHCO_3$, XRD and TGA were performed after carbonation experiment. In order to prove that the captured CO_2 gas is converted into sodium bicarbonate, XRD analysis was performed for the precipitated salts. The XRD results of the carbonated compound generated during carbonation are shown in Figure 4. As it can be observed from the XRD patterns, it was revealed that the majority of the precipitated powder was $NaHCO_3$, with a slight amount of Na_2CO_3 mixed in the powder [14].

The TGA results were used to determine the thermal decomposition characteristics of produced $NaHCO_3$ and calculate its purity. As it can be observed from the TGA pattern in Figure 5, the weight loss began at about 85.0 °C and ended at 182.3 °C which represent the thermal decomposition of $NaHCO_3$ to H_2O and CO_2 according to the reverse reaction of (2) The TGA results show a mass reduction of approximately 30% due to the thermal decomposition of $NaHCO_3$ [15, 16]. The second weight

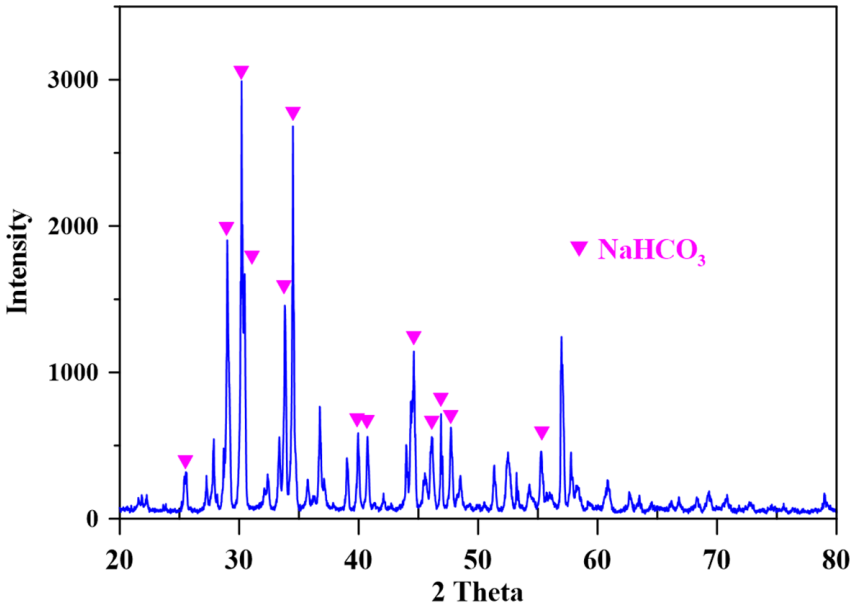

Figure 4. XRD results of the precipitated sodium bicarbonate

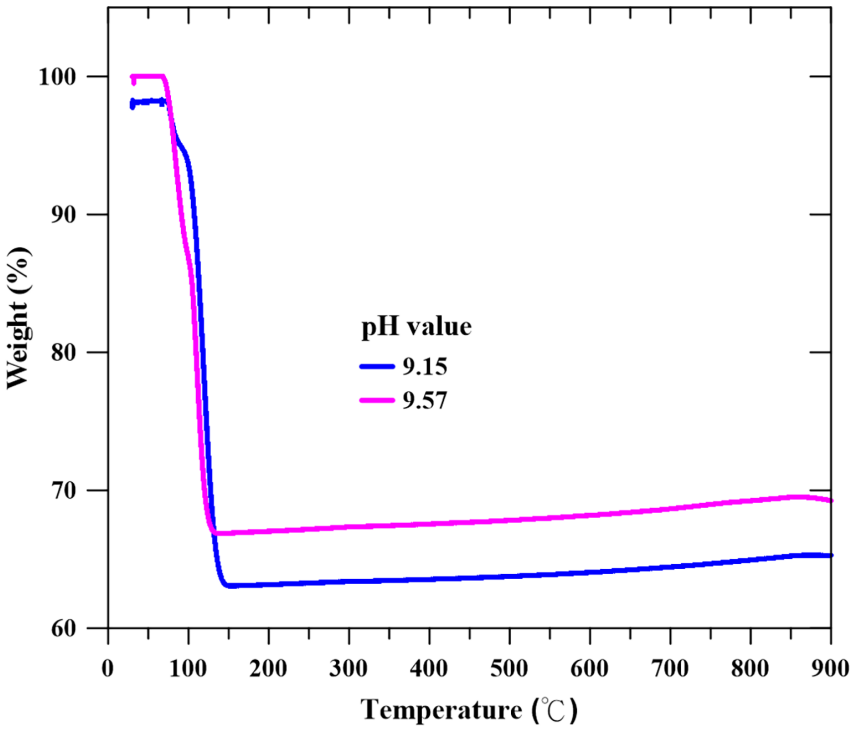

Figure 5. TGA results of the precipitated sodium bicarbonate at different pH values

loss above 825 °C is attributed to the thermal decomposition of Na_2CO_3. Therefore, by examining the weight loss values in the TGA plot, it can be confirmed that the sample corresponds to $NaHCO_3$. The actual mass of $NaHCO_3$ produced is calculated based on the first weight loss observed in the TGA plot, which also provides the purity of the produced $NaHCO_3$. Experimental data reported in this study demonstrate that absorbed CO_2 is effectively converted into sodium carbonate salts, with the purity of the produced $NaHCO_3$ exceeding 95%.

CO_2 capture in packed bed reactor

The CO_2 absorption experiments were conducted in continuous mode, with simulated flue

gas entering counter-currently through a packed column reactor at the bottom and exiting at the top. A gas mixture containing 14 vol% CO_2 was used to simulate emissions from a typical coal-fired power plant, and a 15 wt% aqueous sodium hydroxide solution was used as the absorbent. Prior to commencing the absorption experiments, 2 liters of the absorbent solution were injected into the packed bed reactor. A non-dispersive infrared gas analyzer was used to measure the CO_2 concentration in the gas exiting the reactor to determine the CO_2 capture efficiency. The effects of absorbent flow rate and gas flow rate on CO_2 capture efficiency were investigated, with absorbent solution flow rates ranging from 5 to 15 L/h countercurrent to the gas flow rates of 300 and 500 L/h.

As illustrated in Figure 6, a decrease in CO_2 capture efficiency was observed over time, rapidly reaching a minimum level, indicating near-complete consumption of hydroxide ions in the absorbent solution. At a gas flow rate of 500 L/h, after 120 minutes of experiment, the liquid flowing through the packed bed reactor was saturated with CO_2, and the hydroxide ions were almost entirely consumed. This led to a significant decrease in the CO_2 removal efficiency, regardless of the absorbent flow rate, failing to increase the CO_2 capture efficiency. According to the experimental data, during the first 100 minutes, the gas flow rate did not affect CO_2 capture efficiency, maintaining at 100%. However, after this initial period, all trends showed a substantial decrease in CO_2 capture efficiency, indicating that the absorbent solution was becoming saturated and no longer absorbing CO_2. Over a longer duration (>120 minutes), regardless of the absorbent flow rate, the CO_2 capture efficiency stabilized at around a minimum of 10%.

When the gas flow rate was 300 L/h, the CO_2 removal efficiency remained at 100% for the first 200 minutes. However, after 220 minutes, a sharp decline in CO_2 capture efficiency was observed, which is attributed to the gradual depletion of available hydroxide ions to the minimum level. As the reaction time increases, the CO_2 removal efficiency stabilizes at the minimum of 10% after 300 minutes, indicating that the OH^- ions in the absorbent have been completely consumed during the carbonation reaction. Comparing different gas flow rates, the CO_2 capture efficiency drops rapidly to the minimum at higher flow rates, indicating that the absorbent reaches saturation more quickly. This phenomenon is reasonable, because a higher gas flow rate results in a relatively shorter residence time of the gas through the packing material, causing more CO_2 gas to remain unabsorbed by the absorbent.

Notably, the sudden drop in CO_2 capture efficiency indicates the exhaustion of OH^- ions in the absorbent, which means the packed bed is saturated with CO^2 and further CO_2 absorption has ceased, marking the end of the absorption experiment. To maintain high CO_2 capture rates, it is necessary to periodically replenish the absorbent solution with

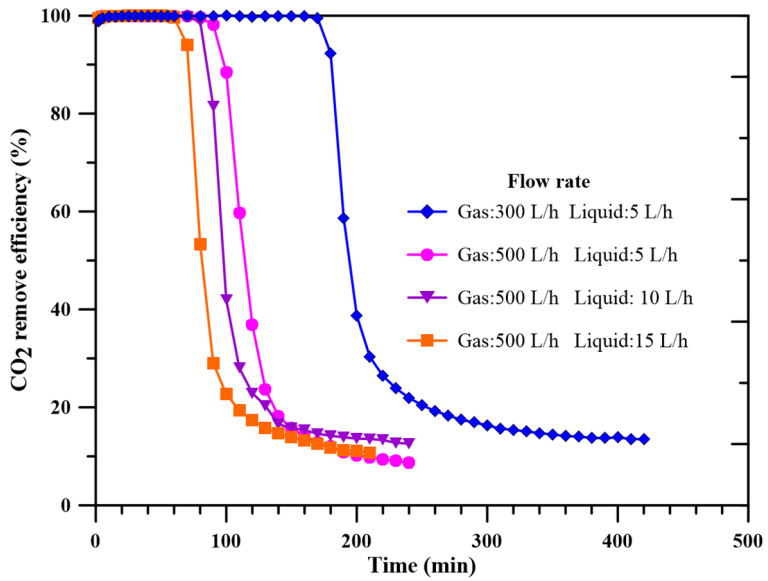

Figure 6. CO2 removal efficiency changes with reaction time. NaOH initial concentration is 15 wt% and CO_2 inlet gas concentration is 14v%

fresh NaOH solution to restore the OH^- ion concentration and maintain the pH above 13, ensuring continued effectiveness in CO_2 removal.

Effect of the gas flow rate in bubble column reactor

In this study, a 15 wt% sodium hydroxide aqueous solution was used as the absorbent, with CO_2 absorption initiating at an initial pH of 14.0, conducted within a bubble column reactor for CO_2 capture and mineral carbonation. In continuous operation, the simulated gas flow was injected in a counter-current manner from the bottom of the column, while the absorbent solution entered the reactor from the top. The bubble column is equipped with a hemisphere gas sparger at the bottom to help uniformly disperse the CO_2 gas within the absorbent solution. The CO_2 capture and mineral carbonation experiments used the same CO_2 composition and absorbent solution, conducted at a fixed flow rate of 5 L/h. The effect of gas flow rate on the pH value of the absorbent solution was investigated by varying the gas flow rate from 300 L/h to 700 L/h, corresponding to superficial gas velocities ranging from 2.95 to 6.9 cm/s.

Figure 7 shows a significant decrease in pH value over time. In the initial stage of the reaction, CO_2 absorption started at a pH of 14.0, with a high concentration of hydroxide ions present. Consequently, most of the CO_2 was rapidly absorbed, leading to a rapid decrease in pH to 13 due to the consumption of the initial alkalinity. During this stage, CO_2 interacts with the sodium hydroxide solution, undergoing successive reactions according to reaction 1 and 2 to form sodium carbonate and sodium bicarbonate. Previous studies [10, 11] suggest that the formation of sodium bicarbonate occurs at a much slower rate compared to the formation of sodium carbonate. As the reaction progresses, hydroxide ions are rapidly consumed, causing the solution to become more acidic, and the pH drops to 11. This phenomenon can be attributed to the fast rate of the carbonation reaction, where most of the absorbed CO_2 reacts with OH^- to produce carbonate ions. Within the pH range of 11 to 13, all pH curves exhibit a similar trend, but the rates of pH decline vary at different gas flow rates, as shown in Figure 7. From the figure, it is evident that higher gas flow rates lead to more CO_2 entering the aqueous solution, increasing the consumption of hydroxide ions in the absorbent and resulting in a sharp pH drop over a shorter period. This trend indicates that increasing the gas flow rate may enhance the mass transfer rate, causing the absorbent to reach saturation quicker and resulting in a more significant decrease in pH. Therefore, it is clear from the figure that the pH drop is much faster at a gas flow rate of 700 L/h compared to 300 L/h and 500 L/h. As the reaction progresses further, due to the slow rate of the bicarbonate reaction, the pH of the absorbent solution changes very little. This slow reaction results in minimal CO_2 absorption by the

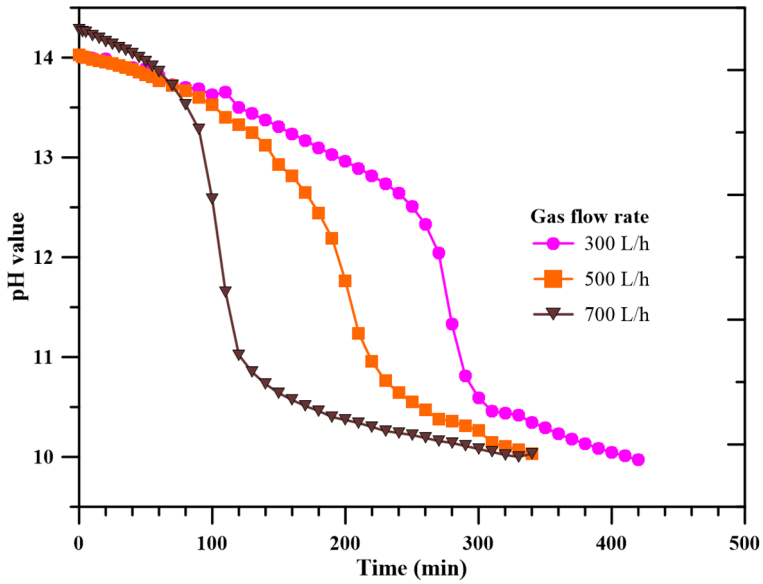

Figure 7. Solution pH value changes with reaction time. NaOH initial concentration is 15 wt% and absorbent flow rate is 5 L/h; CO_2 inlet gas concentration is 14v%

bicarbonate, eventually leading to the absorbent becoming fully saturated with unreacted CO_2. In other words, the characteristic behavior of absorption and mineral carbonation is that the pH remains nearly constant, indicating that the sodium hydroxide absorbent can no longer absorb further CO_2, and the reaction completes at a pH of 10.0.

The experimental results show that the pH curve exhibits an inflection point around 11, after which the pH decreases very slowly until reaching the final pH value of 10.0. This trend remains consistent regardless of the gas flow rate, as shown in Figure 8. Within the pH range of 10 to 11.0, the pH value remains relatively stable, indicating that the absorption process is nearing completion. On the basis of these results, it can be observed that when sodium carbonate reacts with carbon dioxide to produce sodium bicarbonate, the pH drop is less pronounced. This suggests that the reaction involving sodium bicarbonate proceeds at a slower rate compared to other stages of the absorption process.

Effect of the absorbent flow rate in bubble column reactor

This experimental study investigated the effects of different NaOH absorbent flow rates on CO_2 absorption and mineral carbonation in a bubble column reactor. The gas flow rate was held constant at 500 L/h, while the absorbent flow rates were set at 5, 10, 15, and 20 L/h for testing. Figures 8 and 9 show the variations in pH value and CO_2 removal efficiency at different absorbent flow rates, respectively. The pH variation over time is explained by the consumption rate of OH^- ions, which are depleted as CO_2 is absorbed and forms carbonate ions. As the solution becomes saturated with CO_2, the absorption rate decreases, leading to a slower pH reduction. Figure 8 shows a consistent trend in pH variation across all absorbent flow rates from 5 to 20 L/h. At higher flow rates (15 L/h and 20 L/h), the pH drop is more pronounced, indicating a faster carbonation process and quicker saturation of CO_2 absorption. This is due to the increased availability of OH^- ions, which accelerates the carbonation reaction. However, at an absorbent flow rate of 20 L/h, CO_2 absorption reaches its peak, and further increases in flow rate do not significantly improve efficiency, indicating a saturation point. At flow rates below 10 L/h, the diffusion rate of hydroxide ions towards the gas-liquid interface is slower, resulting in a more gradual pH decrease.

Figure 9 shows the variation in CO_2 capture efficiency at different absorbent flow rates. Initially, CO_2 capture efficiency is high, maintaining its maximum value within the first 120 minutes. During this period, the CO_2 removal efficiency exceeds 95% across different flow rates. As carbonation progresses, hydroxide ions react with CO_2 to form carbonate ions, and subsequently sodium carbonate converts to sodium bicarbonate, as described by Equation 3. As it was

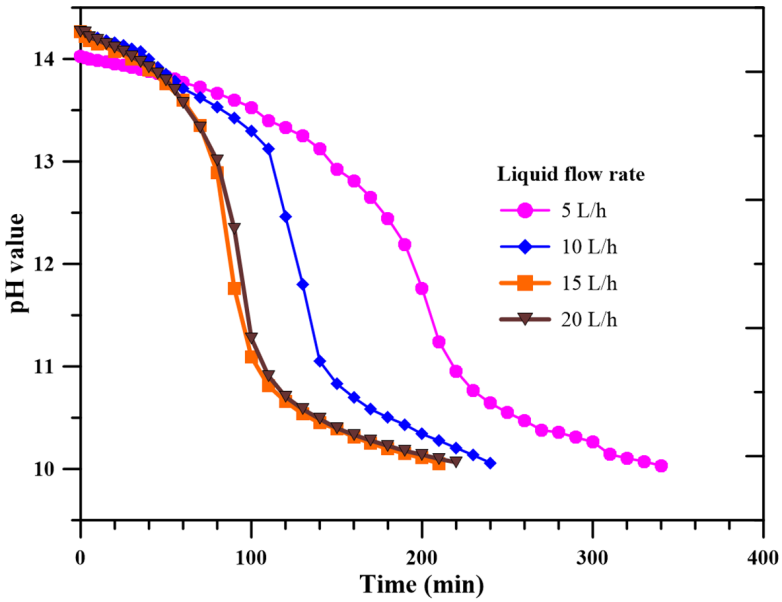

Figure 8. Efficiency of CO_2 captured from gas during the carbonation in NaOH solution. NaOH initial concentration is 15 wt%; CO_2 inlet gas concentration is 14 v% :gas flow rate is 5 L/h

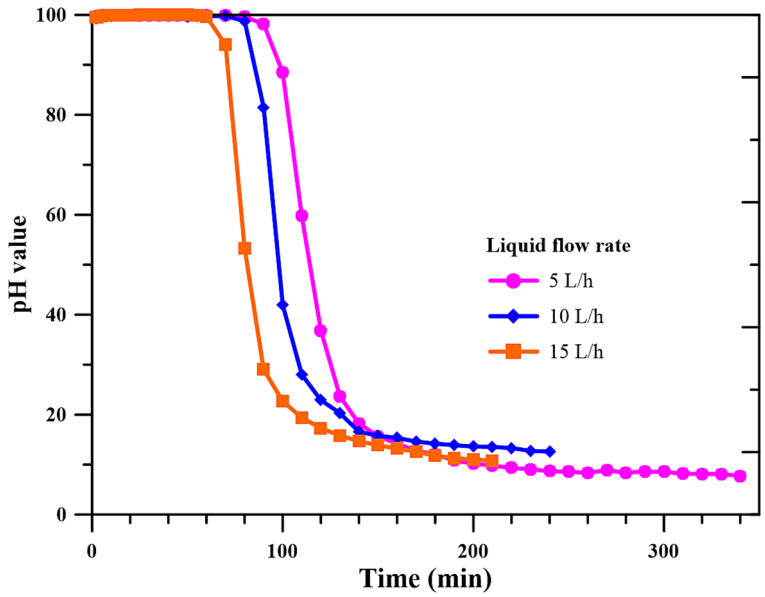

Figure 9. Efficiency of CO_2 capture from gas according to reaction time. NaOH initial concentration is 15 wt%; CO_2 inlet gas concentration is 14 v% :gas flow rate is 500 L/h

mentioned in the previous section, the reaction rate of bi-carbonation is much slower compared to that of carbonation, making this conversion unfavorable for continued CO_2 absorption. Eventually, capture efficiency declines as the solution becomes rich in carbonate and bicarbonate ions. Figure 9 further shows that a decrease in absorbent flow rate accelerates the decline in CO_2 capture efficiency. After 120 minutes, the CO_2 capture efficiency at a flow rate of 5 L/h decreased from 100% to 31%, while at 10 L/h and 15 L/h, it dropped to 23% and 17%, respectively. From 120 to 240 minutes, the capture efficiency rapidly decreased to its lowest point, indicating that the effect of absorbent flow rate diminishes as the solution becomes saturated with CO_2. The study indicated that increasing the absorbent flow rate generally improves CO_2 absorption efficiency up to an optimal point, beyond which no significant improvements are observed. This finding underscores the need for a balanced approach in designing and operating bubble column reactors to achieve efficient CO_2 capture and mineral carbonation processes in the future.

Effect of gas sparger designs in bubble column reactor

The size distributions of bubbles are significantly influenced by the type of gas sparger, thereby impacting hydrodynamics and other parameters relevant to bubble column reactor. This experimental study investigated the effects of sparger design and gas sparger openings in a bubble column reactor for CO_2 absorption in NaOH absorbent. The objective was to evaluate these four different types of spargers to determine which configuration provides the highest CO_2 removal efficiency and optimum hydrodynamics in the bubble column. Figure 10 illustrates the different types of spargers: (a) cone, (b) hemisphere, (c) multi-pipe, and (d) vertical dual-pipe, with their respective properties provided in Table 2. It should be emphasized that the total orifice area for gas sparging is the sum of the areas of all the pipes or spargers.

Cone sparger

As shown in Figure 10a, the cone sparger is constructed from six layers of sintered mesh with

Table 2. Main characteristics of different spargers design

Type of gas sparger	Porous diameter of sparger (μm)	Number of pipes	Total orifice area (m^2)
Cone	500	1	0.0236
Hemisphere	10	1	0.0353
Multi pipe	10	7	0.0380
Vertical dual pipe	1	2	0.0377

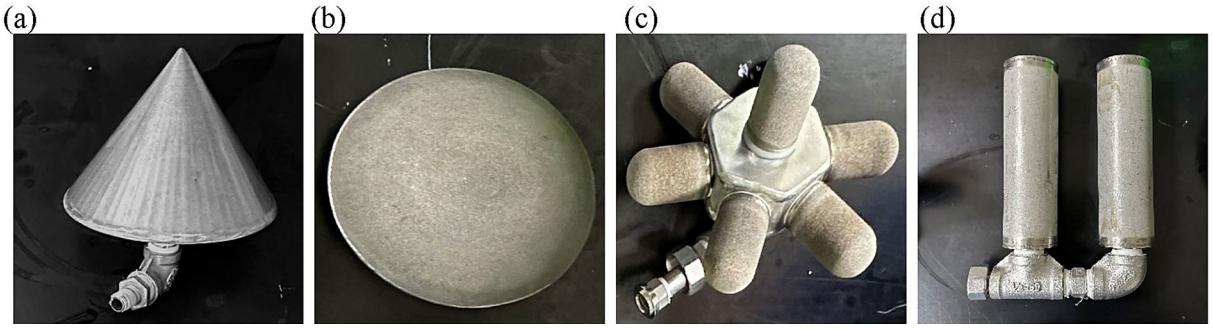

Figure 10. Different types of spargers (a) cone (b) hemisphere (c) multi pipe (d) vertical dual pipe

perforated metal featuring an aperture width of 0.5 mm. It is welded to a circular stainless steel base with a diameter of 0.15 m and a height of 0.10 m. Figure 11a shows that gas bubbles are released axially outward from the apex of the cone, forming a centrally concentrated distribution pattern around the sparger. Compared to the spargers with radial jetting orifices, axial dispersion and channeling flow dispersion are more pronounced, resulting in poorer radial dispersion around the sparger. Figure 12 shows that the cone sparger produces larger bubble diameters and slower liquid recirculation throughout the bubble column, resulting in the lowest CO_2 removal efficiency. Additionally, only a slight increase in the amount of sodium bicarbonate precipitation in the liquid phase was observed, attributed to the slow precipitation of sodium bicarbonate due to a lower specific interfacial area and significantly reduced mass transfer rate. This corresponds to the significantly larger bubble sizes produced by the sintered wire mesh compared to those produced by porous spargers, as the larger gas bubbles ascend rapidly through the column. The main characteristics of the different spargers are shown in Table 2. It was found that the total orifice area for the three spargers, excluding the cone sparger, is of the same order of magnitude. This high orifice area contributes to their high mass transfer efficiency.

Hemisphere sparger

The hemisphere sparger consists of a hemispherical top with microporous orifices, welded to a circular stainless steel base with a diameter of 0.15 meters and extending to a height of 0.102 meters from the base. Notably, the orifices, with a diameter of 10 micrometers, are located only on the top surface of the sparger, with none on the bottom. Figure 11b shows that the hemisphere sparger, with its upward jetting orifices, induces localized liquid recirculation near the sparger, which then propagates smaller recirculation patterns within the reactor. Compared to the cone sparger, the microporous orifice design of the hemisphere sparger offers advantages, potentially improving mass transfer operations in the bubble column and more effectively promoting the precipitation of sodium bicarbonate. As it is shown in Figure 12, the hemisphere sparger with

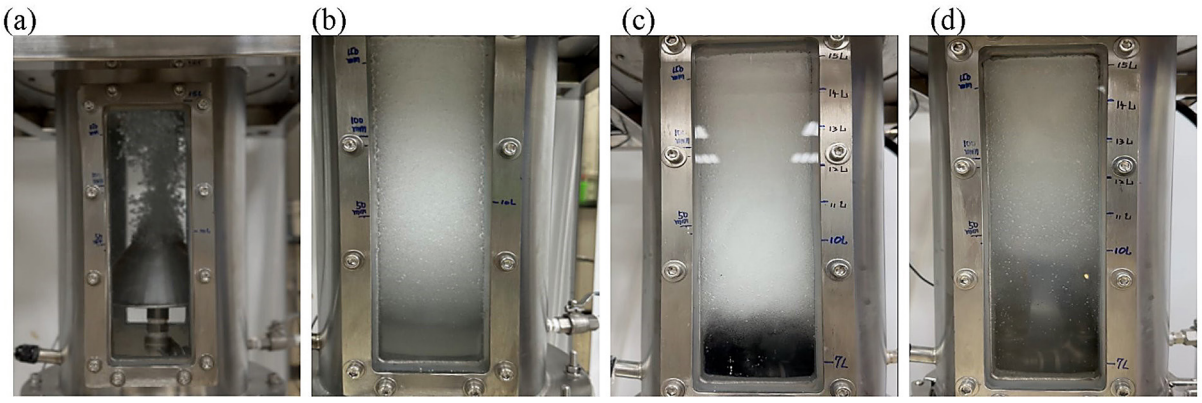

Figure 11. Photographs of flow pattern for different sparger design in bubble column reactor, (a) cone, (b) hemisphere, (c) multi pipe, (d) vertical dual pipe

microporous orifices achieves higher CO_2 removal efficiency compared to the cone sparger with a sintered mesh. The smaller pore diameter, ranging from 10 to 50 micrometers, likely increases the surface area available for gas-phase flow, thereby facilitating more efficient CO_2 removal.

Multi tube sparger

As it is shown in Figure 10c, the multi-pipe sparger consists of six stainless steel porous pipes with a diameter of 0.16 meters, threaded into a hexagonal disk body. Additionally, a vertical porous pipe is installed at the center of the hexagonal disk body. These microporous pipes, with a pore size of 10 micrometers, are specifically designed to produce very fine bubbles and ensure their even dispersion in all directions. The sparger with vertical radial jetting orifices achieves a more uniform radial dispersion of the bubbles. This design facilitates the ascent of gas bubbles from both the radial horizontal and central vertical porous pipes, ensuring uniform gas distribution throughout the bubble column reactor. The results in Figure 11(c) show that the multi-pipe sparger combined with the vertical porous pipe significantly enhances CO_2 capture using NaOH absorbent in the bubble column reactor compared to the spargers with only upward diffusing orifices. Additionally, it demonstrates increased mixing provided by the bubble jets created from the radial dispersion orifices, thereby also promoting the formation of precipitated sodium bicarbonate. Figure 12(c) further shows that the vertical pipe has additional diffusers on the side face, enhancing mixing around the sparger. This significantly improves mass transfer efficiency in the bubble column, greatly increasing CO_2 removal efficiency.

Vertical dual pipe sparger

The vertical dual-pipe sparger is designed with two vertical pipes, each with a pore size of 1 micrometer, specifically for generating ultrafine bubbles. It has been observed that this microporous sparger can produce a large volume of bubbles that remain in the bubble column for an extended period. In its simple design, all orifices are located on the side of the sparger to enhance radial mixing around it. The radial bubble jets aim to promote the ascent of any solid particles near the sparger, reducing the blockage of the microporous openings. Figure 11d illustrates that the vertical dual-pipe sparger has a similar effect to the multi-pipe sparger with vertical porous pipe, enhancing radial dispersion as bubbles diffuse from its sides. This advantage may be due to the significant impact of bubble jets on radial distribution, resulting in notable radial bubble distribution around the sparger. Figure 11(d) shows that both the vertical dual-pipe sparger and the multi-pipe sparger with a vertical porous pipe exhibit

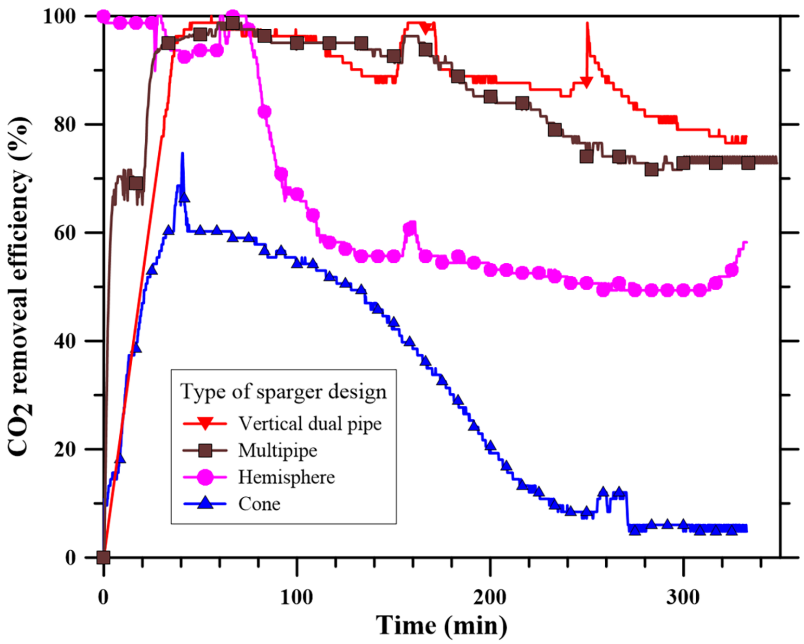

Figure 12. The CO_2 capture efficiency for different types of spargers: (a) cone, (b) hemisphere, (c) multi-pipe, and (d) vertical dual-pipe

excellent performance, leading to increased sodium bicarbonate precipitation in the bubble column reactor. Further results in Figure 12 demonstrate that the vertical dual-pipe sparger with ultra-fine openings, by providing a higher specific surface area and thus enhanced mass transfer efficiency, exhibits superior performance, achieving the highest CO_2 removal carbonation efficiency and the highest purity of sodium bicarbonate.

The experimental results observed that the spargers with smaller orifices performed better, as they could produce a large volume of bubbles that remained in the column for a longer duration, thereby promoting the carbonation reaction to form sodium bicarbonate. Both the multi-pipe sparger and the vertical dual-pipe sparger have vertical gas diffusion designs that exhibit radial distribution of gas, enhancing mass transfer during the gas-liquid carbonation reaction in the bubble column. The experimental results also showed that the spargers with vertical porous pipes achieved high CO_2 removal efficiency and high sodium bicarbonate purity, with CO_2 removal efficiency consistently maintained above 90% and the product purity reaching 95% sodium bicarbonate. It is evident that the design of the sparger significantly affects the recirculation patterns between gas and liquid in the bubble column, which helps in enhancing the mixing of CO_2 gas. The results obtained in this experiment provide extremely useful information for the design and construction of pilot-scale facilities.

CONCLUSIONS

Under bench-scale experiments, the effects of various parameters on CO_2 capture performance were studied, including inlet gas flow rate, absorbent flow rate, solution pH value, and gas sparger design. Initially, the study examined the impact of operating parameters on CO_2 removal efficiency using a packed bed. It was observed that increasing gas flow rates beyond 500 L/h resulted in a significant decrease in CO_2 removal performance, whereas raising the absorbent flow rate yielded a marginal improvement. Subsequently, the same operating parameters were varied to analyze their influence on absorption efficiency in the bubble column reactor. Bicarbonate precipitation, as a continuous process in the bubble column reactor, involves pumping flue gas into a solution of sodium carbonate and sodium bicarbonate to precipitate bicarbonate crystals. Similar to the packed bed column, an increase in gas flow rates notably boosted efficiency, with the absorbent flow rate demonstrating a more pronounced impact. Additionally, elevating the liquid flow rate effectively delayed the saturation of the absorbent, having the most substantial impact on the CO_2 removal efficiency.

The experiments highlighted the pH value of the liquid absorbent as the most critical operating parameter. Maintaining a pH value within the range of 8.5–9.5 in the bubble column was recommended for achieving high CO_2 removal efficiency and $NaHCO_3$ purity levels exceeding 95%. The study showcased how vertical gas diffusion design enhanced mass transfer between gas and liquid, creating unique radial distribution patterns and improving liquid circulation within the reactor. Additionally, efficient gas sparger design accelerated the bi-carbonation reaction, thereby enhancing $NaHCO_3$ precipitation in the bubble column.

Regarding the hazards associated with the large-scale use of NaOH, attention should be directed toward the risks of acute exposure during operation. NaOH is a highly caustic substance widely used across various industrial sectors. The primary risks to workers arise from acute exposure, which can lead to severe chemical burns, respiratory irritation, and eye damage. Although sodium hydroxide has a low vapor pressure, limiting significant emissions to the terrestrial environment, inhalation exposure remains the most concerning route for workers. To mitigate the occupational exposure to NaOH, the use of personal protective equipment is assumed to reduce the actual risks. However, the effectiveness of such measures largely depends on site-specific management practices, procedures, and worker training. In terms of administrative controls, the following procedures should be implemented to minimize exposure: proper storage of NaOH to prevent accidental spills, regular maintenance, and inspection of equipment to avoid leaks. By integrating these strategies—personal protective equipment, engineering controls, administrative practices, and continuous monitoring—the occupational exposure to NaOH can be significantly reduced, ensuring the safety of workers from potential hazards.

For the future development of this technology, a cooperative agreement program was executed to evaluate the potential of carbon capture for steam boiler plants at the Taisugar factory in Tainan City, Taiwan. A pilot-scale CO_2 mineral

carbonation process was established as a CO_2 capture field test facility, capable of capturing CO_2 from various industrial flue gases. To demonstrate continuous operation, the pilot-scale carbonation process was conducted over 5 days, where flue gas containing 8% CO_2 was fed into packed columns and a bubble column in series. A 15% NaOH solution reacted counter-currently with the CO_2 to form $NaHCO_3$. The pilot plant demonstrated a capacity to capture more than 95% of the CO_2 from a slipstream of the natural gas steam boiler, which equates to capturing approximately 10 kg/day of CO_2 and producing 12 kg/day of $NaHCO_3$ as the mineralization product. The results of this pilot test proved that the CO_2 mineral carbonation and utilization process is technically feasible on a large scale. However, transitioning from pilot scale to commercial-scale demonstration requires certain adjustments. To improve the long-term process, it is essential to address two technical challenges: bicarbonate precipitation and bubble size. Notably, smaller bubbles result in the formation of larger bicarbonate crystals due to the increased surface area available for the gas-liquid reaction. However, smaller bubbles also lead to the production of a large number of fine bicarbonate crystals, which could potentially clog the sparger orifice.

Furthermore, continuous bubble flow must be optimized to prevent gas sparger plugging by solid particles, while ensuring that the bubble jets can lift any solid particles effectively. During the field tests at the pilot plant, it was observed that the bicarbonate crystals produced in the bubble column reactor contributed to sparger orifice blockages, leading to slow liquid circulation and inhibiting $NaHCO_3$ production. This issue was resolved by replacing the sparger, which resulted in the creation of smaller bubbles and faster liquid circulation within the bubble column reactor.

For future work, further study on the kinetics of bicarbonate precipitation is critical to effectively control the formation of bicarbonate crystals in the bubble column of saturated carbonate solutions.

Acknowledgment

The authors would like to thank the National Science and Technology Council of the Republic of China, Taiwan, for financially supporting this research under contract no. MOST 111-3111-Y-042A-006.

REFERENCES

1. Intergovernmental Panel on Climate Change (IPCC). AR5 Synthesis Report: Climate Change (2014), Geneva, Switzerland, AR5 Synthesis Report: Climate Change 2014 — IPCC.
2. Olajire A.A. (2010). CO_2 capture and separation technologies for end-of-pipe applications - A review. *Energy, 35*, 2610–2628. https://doi.org/10.1016/j.energy.2010.02.030
3. Lee J.H., Kwak N.S., Lee I.Y. (2015). Performance and economic analysis of commercial-scale coal-fired power plant with post-combustion CO_2 capture. *Korean J. Chem. Eng. 32*, 800–807. https://doi.org/10.1007/s11814-014-0267-0
4. Wang M., Lawal A., Stephenson P., Sidders J. Ramshaw C. (2011). Post-combustion CO_2 capture with chemical absorption: a state-of-the-art review. *Chem. Eng. Res. Des. 89*, 1609–1624. https://doi.org/10.1016/j.cherd.2010.11.005
5. Markewitz P., Kuckshinrichs W., Leitner W., Linssen J., Zapp P., Bongartz R., Schreiber A., Müller T. E. (2012). Worldwide innovations in the development of carbon capture technologies and the utilization of CO_2, *Energy Environ. Sci. 5*(6), 7281–7305. https://doi.org/10.1039/C2EE03403D
6. Shim J.G., Lee D.W., Lee J.H., Kwak N.S. (2016). Experimental study on capture of carbon dioxide and production of sodium bicarbonate from sodium hydroxide. *Environ. Eng. Res. 21*, 297–303. https://doi.org/10.4491/eer.2016.042
7. M. Yoo, S.J. Han, J.H. (2013). Wee, Carbon dioxide capture capacity of sodium hydroxide aqueous solution. *J. of Environ. Management. 114*, 512–519. https://doi.org/10.1016/j.jenvman.2012.10.061
8. Guo Y., Niu Z., Lin W. (2011). Comparison of removal efficiencies of carbon dioxide between aqueous ammonia and NaOH solution in a fine spray column. *Energy Procedia 4*, 512–518. https://doi.org/10.1016/j.egypro.2011.01.082
9. Kordylewski W., Sawicka D., Falkowski T. (2013). Laboratory tests on the efficiency of carbon dioxide capture from gases in NaOH solutions. *J. of Ecol. Eng. 14*, 54–62. https://doi.org/10.5604/2081139X.1043185
10. Joe J., Clive B., Mark C., Al Y., David L. (2010). SkyMine Carbon, Mineralization Pilot Project. United States.
11. Han S.J., Yoo M., Kim D.W., Wee J.H. (2011). Carbon dioxide capture using calcium hydroxide aqueous solution as the absorbent. *Energy Fuels 25*, 3825–3834. https://doi.org/10.1021/ef200415p
12. Mahmoudkhani M., Keith D.W. (2009). Low-energy sodium hydroxide recovery for CO_2 capture from atmospheric air thermodynamic analysis.

Int. J. Greenh. Gas Con. 3, 376–384. https://doi.org/10.1016/j.ijggc.2009.02.003

13. Cousins A., Wardhaugh L.T., Feron P.H.M. (2011). A survey of process flow sheet modifications for energy efficient CO_2 capture from flue gases using chemical absorption. *Int. J. Greenh. Gas Con. 5*, 605–619. https://doi.org/10.1016/j.ijggc.2011.01.002
14. Pozzo A.D., Moricone R., Tugnoli A., Cozzani V. (2019). Experimental investigation of the reactivity of sodium bicarbonate toward hydrogen chloride and sulfur dioxide at low temperatures Ind. *Eng. Chem. Res. 58*, 6316–6324. https://doi.org/10.1021/acs.iecr.9b00610
15. Chen X.K., Lu K.L., Xiao Y., Su B., Wang Y.Y., Zhao T.L. (2022). Investigation on the inhibition of aluminum dust explosion by sodium bicarbonate and its solid product sodium carbonate. *ACS Omega, 7*(1), 617–628. https://doi.org/10.1021/acsomega.1c05224
16. Keener T.C., Frazier G.C., Davis W.T. (1985). Thermal decomposition of sodium bicarbonate. *Chem. Eng. Commun. 33*, 93–105. https://doi.org/10.1080/00986448508911162